ACS OMEGA

http://pubs.acs.org/journal/acsodf

Article

Vibrational Optical Activity Study of Four Antibiotic (Lipo)glycopeptides: Vancomycin, Oritavancin, Dalbavancin, and Teicoplanin

Roy Aerts,* Jonathan Bogaerts, Christian Johannessen, and Wouter A. Herrebout

Cite This: *ACS Omega* 2022, 7, 43657−43664

Read Online

ACCESS | Metrics & More | Article Recommendations | Supporting Information

ABSTRACT: The antibiotic glycopeptide class, of which vancomycin is the original compound, has received due attention over the past few decades in search of antibiotics to overcome resistances developed by bacteria. Crucial for the understanding and further development of glycopeptides that possess desired antibacterial effects is the determination of their conformational behavior, as this sheds light on the mechanism of action of the compound. Among others, vibrational optical activity (VOA) techniques (vibrational circular dichroism and Raman optical activity) can be deployed for this, but the question remains to what extent these spectroscopic techniques can provide information concerning the molecular class under investigation. This contribution takes the last hurdle in the search for the capabilities of the VOA techniques in the conformational analysis of the antibiotic glycopeptide class by extending research that was previously conducted for vancomycin toward its three derivatives: oritavancin, dalbavancin, and teicoplanin. The principal information that can be drawn from VOA spectra is the conformation of the rigid cyclic parts of the glycopeptides and the aromatic rings that are part hereof. The addition or removal of carbohydrates does not induce noticeable VOA spectral responses, preventing the determination of the conformation they adopt.

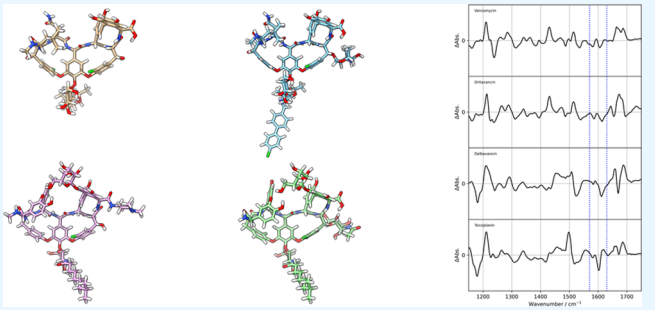

INTRODUCTION

Vancomycin is an antibiotic glycopeptide and was isolated for the first time in 1956 from *Streptomyces orientalis*.[1] As vancomycin has been around for quite a while now, its mechanism of action has been extensively studied, which involves the determination of the compound's conformational behavior and in what molecular interactions it engages with the biological target. By means of X-ray diffraction (XRD) and NMR, vancomycin was determined to enclose the D-Ala-D-Ala peptide sequence of the bacterial cell wall precursor lipid II, hampering the construction of the cell wall.[2−5]

As is the case for any antibiotic agent, resistance mechanisms develop sooner or later. Presently, resistance toward existing antibiotics is accumulating, risking becoming an increasing global threat during the upcoming decades.[6] The first vancomycin-resistant bacterial stains surfaced by 1986.[7] Nevertheless, resistance that has been developed so far can be circumvented by switching to the derivatives of vancomycin. By altering the chemical structure, different interactions with the biological target are unlocked, oftentimes accompanied by changes in the overall conformation of the drug compound. Thus, the pharmaceutical activity can be re-enhanced by increased interaction with the biological target and/or by (additional) different mechanisms of action that come into play. Plenty of efforts are therefore made in the synthesis and activity testing of novel antibiotic glycopeptides.[8−19] When promising alternatives are discovered, it is of great value to eventually comprehend how this new compound acts, conformation- and interaction-wise, as this provides us with the necessary luggage to face ever-changing nature.

Besides methods such as XRD and NMR, which are routinely used for determining the conformation and interaction of systems, IR- and Raman-based techniques can aid in this puzzle. Especially the vibrational optical activity (VOA) techniques, which are based on the differential Raman scattering (Raman optical activity, ROA) or IR absorption (vibrational circular dichroism, VCD) of left and right circular polarized photons by chiral systems, are useful due to their sensitivity toward the conformational behavior of the compound. The prime example hereof is the identification of the secondary structure of proteins based on ROA marker bands.[20−22] The possibility to calculate VOA intensities and the increasing computational power has boosted the utility of

Received: July 20, 2022
Accepted: November 4, 2022
Published: November 17, 2022

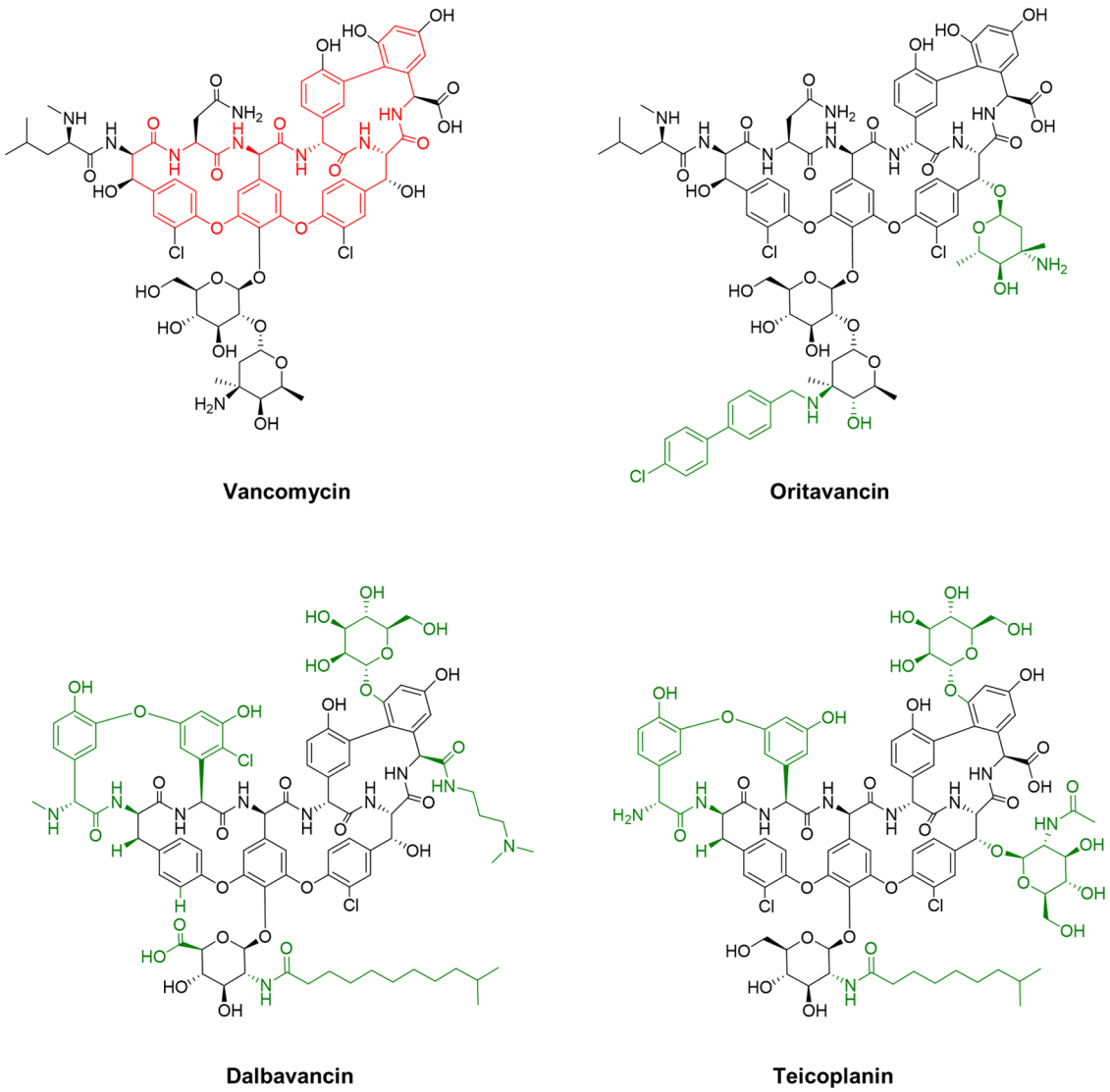

Figure 1. Chemical structures of the antibiotic glycopeptides vancomycin, oritavancin, dalbavancin, and teicoplanin. The molecular parts that set the derivatives structurally apart from vancomycin are indicated in green. The part that is common among all of the compounds is indicated in red color in the drawing of vancomycin.

VOA spectroscopy, as now the spectral intensities could be directly related to the conformational behavior of the studied compounds.[23] Only recently were calculations doable for a compound like vancomycin. We, thereupon, reported the conformational behavior and the interaction of vancomycin with lipid II examined by means of VOA spectroscopy.[24−26] Various conclusions were drawn during these studies regarding the conformational information that could be extracted from the VOA spectra for vancomycin.

In this contribution, we extend the investigation toward several derivatives so as to gain a deeper insight into what the VOA techniques can or cannot tell us about glycopeptide antibiotics. Three derivatives—oritavancin, dalbavancin, and teicoplanin—were selected as subjects of this study (see Figure 1) based on findings for vancomycin: the domination of the aromatic part in the VOA intensities and the invisibility of the carbohydrate entities.[24,25] Oritavancin and dalbavancin are registered as treatment drugs against skin infections since 2014, whereas teicoplanin was approved in 1988 in Europe as a treatment against, among others, bone and soft tissue infections.[27,28] All of the derivatives consist of additional aromatics systems: oritavancin contains a flexible chlorobiphenylmethyl group attached to the 4-*epi*-vancosamine carbohydrate, while dalbavancin and teicoplanin possess two additional aromatic rings that constitute an additional cycle between the first and third amino acids in the peptidic backbone. Oritavancin has an additional aminated sugar attached to the sixth amino acid. Dalbavancin and teicoplanin lack the vancosamine group but have, respectively, one and two carbohydrate groups attached elsewhere. They are actually called lipoglycopeptides, as they contain additional lipophilic side chains, altering the pharmacokinetic and/or pharmacodynamic profile.[27]

Nowadays, the trend in chiroptical spectroscopy is to concentrate on computational work and the analysis thereof. The strength of simulated spectra for the interpretation of experiments is exemplified by our previous work on vancomycin.[24,25] The approach here, during the chiroptical analysis, extends to the derivatives of vancomycin; however, the computational discussion is limited to a minimum. The aim of this contribution is not to completely unravel each of the derivative's spectra and extract the conformational

https://doi.org/10.1021/acsomega.2c04584
ACS Omega 2022, 7, 43657−43664

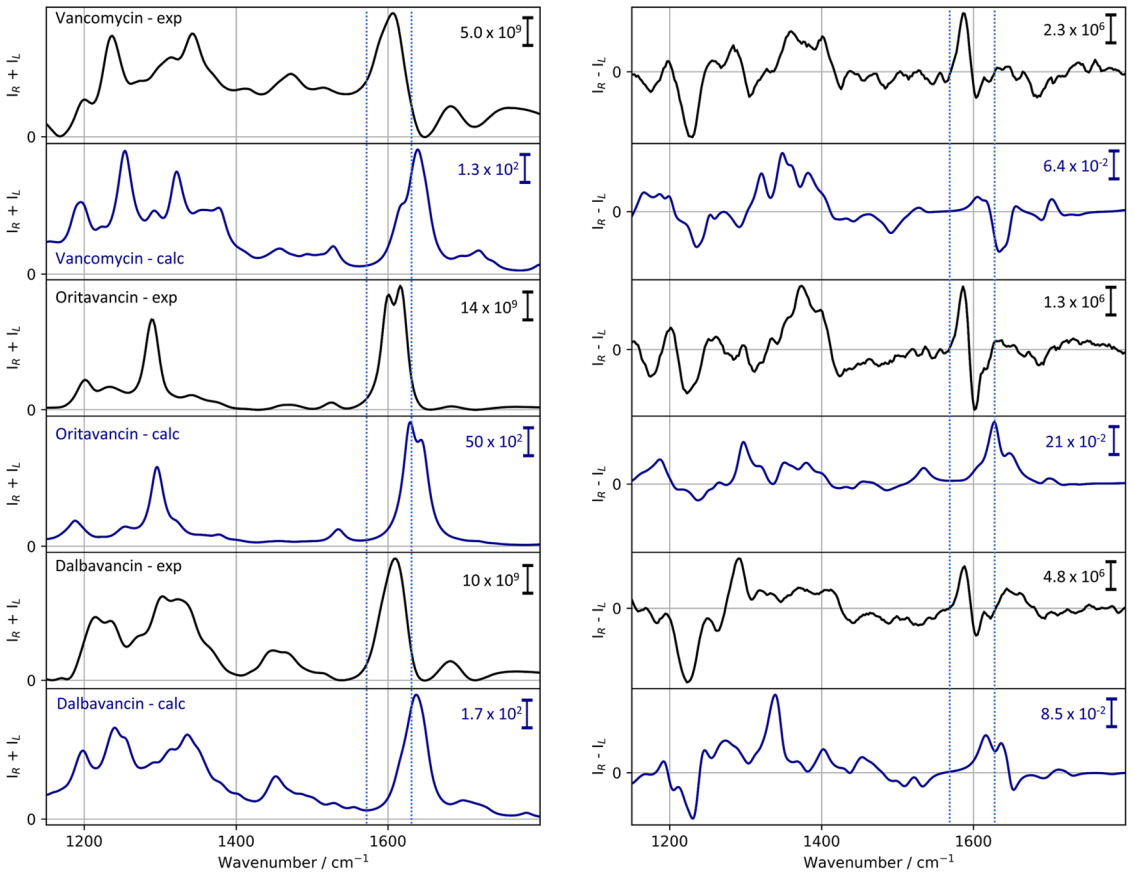

Figure 2. Experimental (black) and calculated (blue) Raman (left) and Raman optical activity (right) spectra of vancomycin, oritavancin, and dalbavancin in aqueous solution. A horizontal scaling factor of 0.987 was applied for the calculated spectra. Spectra for teicoplanin are not reported, as an adequate recording was impossible. The blue dashed lines indicate the borders of the spectral regions that are being discussed separately. As the IR and VCD (see Figure 3) are recorded in DMSO-d_6, only a spectral range down to ∼1150 cm^{-1} is available. In aqueous solution, a larger spectral region is available to prevent confusion, and as the discussion does not highlight any signals below 1150 cm^{-1}, the spectral region is kept identical. Figure S3 (Supporting Information) contains the full spectral range of the aqueous solution recordings.

ensemble but rather to attempt to understand why certain spectral effects are observed upon chemical modification of vancomycin.

METHODOLOGY

Experimental Recordings. Vancomycin (Ambeed), oritavancin (Sigma-Aldrich), dalbavancin (Selleckchem), and teicoplanin (Selleckchem) were purchased from commercial vendors and used without further purification. All solution concentrations were 30 mg mL^{-1}, resulting in an IR absorbance maximum of around 0.6−0.9 absorbance units. This concentration is also adequate for recording high-quality Raman and ROA measurements. The measurements happened at room temperature.

The Raman and ROA measurements were performed in an acetate buffer with a pH of 3.6, required for the solvation of the (lipo)glycopeptides in aqueous solution. A ChiralRAMAN-2X scattered circular polarization (SCP) ROA instrument (Biotools, Inc.) was used for the Raman and ROA recordings. The resolution of this instrument was 7 cm^{-1}. The laser excitation wavelength was 532 nm and the power at the source varied around 800 mW. The total measurement time was 48 h with a single scan illumination time of 2.2 s. The final Raman spectra were obtained after solvent subtraction and Boelens et al. baseline correction.[29] Post-processing the ROA spectrum involved smoothing with a third-order nine-point Savitsky-Golay filter.

DMSO-d_6 was the solvent during the IR and VCD measurements of the four compounds. The switch to this solvent system with respect to the Raman and ROA measurement samples was valid, as the conformation of the glycopeptides was not influenced.[25] This was confirmed by the absence of spectral changes in the experimental Raman and ROA spectra for vancomycin and oritavancin when the solvent was altered (see Figure S1 in the Supporting Information). Teicoplanin did not dissolve to a sufficient degree in the acetate buffer to obtain high-quality spectra with a required signal-to-noise ratio. DMSO-d_6 Raman and ROA recordings of dalbavancin and teicoplanin were attempted but were not successful due to too strong fluorescence effects swamping the Raman and ROA signals. A Bruker Invenio FT-IR spectrometer equipped with a PMA 50 unit with a resolution of 4 cm^{-1} was used for the recordings. The sample cell had a path length of 200 μm and BaF_2 windows. The total recording times for the IR and VCD spectra were 320 scans (∼5 min of acquisition time) and 24 blocks of 3840 scans (∼1 day of total acquisition time), respectively. Solvent subtraction was performed on the sample IR and VCD spectra with solvent measurements under identical conditions.

Computational Details. The three-dimensional (3D) structure and the corresponding VOA spectra of vancomycin

https://doi.org/10.1021/acsomega.2c04584
ACS Omega 2022, 7, 43657−43664

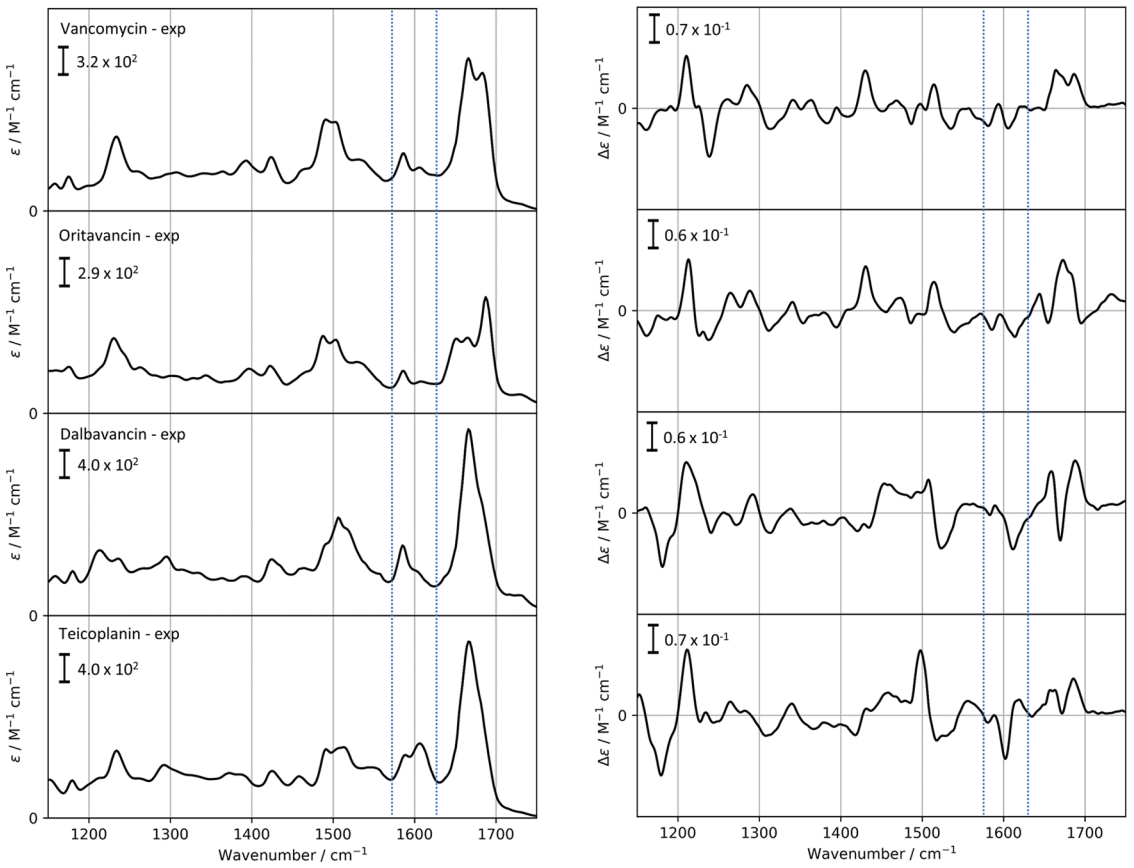

Figure 3. Experimental IR (left) and vibrational circular dichroism (right) spectra of vancomycin, oritavancin, dalbavancin, and teicoplanin in DMSO-d_6. The blue dashed lines indicate the borders of the spectral regions that are being discussed separately. The noise levels of the VCD spectra are negligible.

were adopted from previous work, where the conformation originated from an NMR study and was optimized at a density functional theory (DFT)-level with B3PW91 as the functional and 6-31++G(d,p) as the basis set.[24,25,30] The input structure for oritavancin was created by modifying vancomycin to oritavancin using Gaussview version 6,[31] starting from the aforementioned optimized 3D structure of vancomycin. This ensured that the identical chemical parts' conformation remained highly similar for the two glycopeptides. The 3D structure of teicoplanin was adopted from the 6TOV entry of the Protein Data Bank (PDB), which was a crystal structure of teicoplanin aglycon.[32] The missing chemical entities were manually added using Gaussview 6. Dalbavancin's core structure was identical to that of teicoplanin, and the 3D structure of teicoplanin was modified to form dalbavancin. All of the obtained structures were first geometrically optimized using the DFT method in two steps: the first optimization was performed at the B3PW91/6-31G(d,p) level of theory followed by the second optimization at the B3PW91/6-31++G(d,p) level of theory. All of the DFT-level calculations were performed using Gaussian 16, revision A.03.[33] The geometries were checked to be at a minimum of the potential energy surface by calculating the Hessian at the according level of theory. When so, spectral calculations were performed by calculating the Hessian, Raman, and ROA tensors and the dipole and rotational strength. A scaling factor of 0.987 was applied to the obtained frequencies, which is the routine for correcting overestimations introduced by the harmonic approximation and the usage of a finite basis set.[34] To convert the calculated line spectra into line-broadened spectra, the Raman and ROA intensities were first temperature-corrected (298 K) and line-broadened thereafter using a Lorentzian line broadening with a full width at half-maximum (FWHM) of 20 cm^{-1}. The line broadening of the IR and VCD spectra also involved Lorentzian line broadening, albeit with an FWHM of 10 cm^{-1}. The solvent was implicitly taken into account during all of the DFT calculations using the integral equation formalism model (IEFPCM) as implemented in Gaussian 16. The overlap integral (S_{fg}) was used as a quantitative measure throughout the spectral analysis, calculated as indicated in Section S4 (Supporting Information).

RESULTS

It was found that when the calculated Raman and ROA spectra were compared with experimental ones, the geometry behind the calculations represented well the actual conformation vancomycin adopted.[24] When the calculated Raman and ROA spectra of vancomycin, oritavancin, and dalbavancin, shown in Figure 2 (1150−1800 cm^{-1}) and Figure S3 (Supporting Information; 500−1800 cm^{-1}), are inspected, a good visual match is found with the corresponding experimental recordings for vancomycin and dalbavancin. This is confirmed by an overlap integral, calculated over the spectral region of 500−1800 cm^{-1}, close to 0.8 and 0.5 for the Raman and ROA spectra, respectively, values that are considered adequate for this molecular class.[24,25] The calculated ROA spectrum of oritavancin deviates stronger from the experiment (S_{fg} = 0.18). The conformation of the molecular scaffold of oritavancin,

https://doi.org/10.1021/acsomega.2c04584
ACS Omega 2022, 7, 43657−43664

however, will not differ significantly from that of vancomycin. Correcting the ROA calculation or unraveling the reason for the stronger deviation is, however, beyond the scope of this contribution, as the overall scope is not to determine the precise conformational ensemble of the derivative compounds.

In contrast, the calculated IR and VCD spectra are far from comparable to the experiments (see Figures 3 and S2 in the Supporting Information); a problem we stumbled upon earlier that cannot be overcome.[25] The IR and VCD calculations will therefore play no further role in this article.

In what follows, all of the experimental spectra will be addressed simultaneously, according to certain spectral regions: above 1630 cm^{-1}, between 1570 and 1630 cm^{-1}, and below 1570 cm^{-1}. Note that the spectral range for the aqueous solution recordings is truncated to match the available spectral range of the DMSO-d_6 recordings, as only signals will be highlighted and discussed in this truncated spectral region. The full spectral region of recordings in aqueous solution can be consulted in Figure S3 (Supporting Information). Finally, the spectra are qualitatively discussed and supported by the quantitative overlap integral measure. The values for all of the overlap integrals are reported in Section S4 in the Supporting Information and are reiterated here where necessary.

Amide I Region: >1630 cm^{-1}. Our analysis begins at the amide I spectral region (above ∼1630 cm^{-1}), where signals arise from the carbonyl stretch vibrations. Weak Raman and ROA intensities are observed in this region (see Figure 2), from which no actual structural information can be extracted for the (lipo)glycopeptides.

In contrast, the IR and VCD amide I bands exhibit strong intensities (see Figure 3). All of the IR amide I bands can be described in terms of the three peak positions, most easily observed for oritavancin: ∼1650, ∼1665, and ∼1689 cm^{-1}. For vancomycin, two maxima are present, with almost identical IR intensity, around 1665 and 1689 cm^{-1}. Weak shoulders can be observed below 1665 cm^{-1}. Next, oritavancin exhibits a lower relative intensity at ∼1665 cm^{-1}, and three peaks appear. The amide I region for dalbavancin and teicoplanin is identical (S_{fg} = 1.00; Table S8), with a band centered around 1665 cm^{-1} with shoulders on both sides. The same categorization can be made based on the VCD amide I patterns (see Figure 3). The amide I region for vancomycin is entirely positive, with two maxima around 1664 and 1688 cm^{-1}, whereas the VCD of oritavancin follows a +/−/+/+ pattern. A +/−/+ VCD pattern is observed for dalbavancin and teicoplanin around 1675 cm^{-1}. Even though the general VCD trends for vancomycin and oritavancin are similar, the band shape is different, as was the case for the IR spectra. The spectral split-up of dalbavancin and teicoplanin with respect to the other two compounds is attributable to on the one hand the amount of carbonyl moieties (nine with respect to seven) and on the other hand the nature of the vibrational modes being influenced by the presence of additional aromatic rings in the vicinity of the peptidic backbone, as well as an actual conformational change in the peptidic backbone due to the presence of the additional aromatic rings (see geometries Sections S5 and S6 in the Supporting Information). The difference observed between the amide I of vancomycin and oritavancin is not immediately explainable. Perhaps the presence of 4-*epi*-vancosamine on the sixth amino acid residue influences the nearby carbonyl vibrations.

Aromatic Region: 1570−1630 cm^{-1}. The next important region is located between 1570 and 1630 cm^{-1}, containing aromatic vibrational modes. Strong-intensity Raman and ROA bands are generally observed for all of the (lipo)glycopeptides. Especially the Raman band of oritavancin stands out, carrying a high relative intensity with respect to the remainder of the spectrum (a zoomed-in version of the Raman spectrum of oritavancin can be consulted in Figure S4 in the Supporting Information). This is the result of the presence of two highly Raman active normal mode vibrations among all of the aromatic ring vibrational modes, observable in the corresponding calculations, originating from the chlorobiphenylmethyl entity, unique to oritavancin. The presence of the two intense chlorobiphenylmethyl normal modes overshadows the other aromatic ring Raman intensities in that spectral region, delivering a couplet band rather than a broad Raman band with shoulders, as is the case for both vancomycin and dalbavancin. The other aromatic rings (five for vancomycin and oritavancin and seven for dalbavancin) display Raman intensities in the order of magnitude of the remainder of the spectrum. The shape of the ROA bands in the 1570−1630 cm^{-1} spectral region is similar for all three compounds: a +/− couplet centered around 1600 cm^{-1}. The fact that there is no ROA spectral difference is a result of the ROA intensities that compensate in that spectral region, i.e., positive and negative overlapping signals arising from the chlorobiphenylmethyl entity that is conformationally flexible in solution.[35] The opposite effect is observed for dalbavancin, where the addition of two aromatic rings in a rigid conformation does induce spectral alterations.

Small IR intensities are observed in the aromatic region, with two peaks around 1590 and 1610 cm^{-1} (see Figure 3). Teicoplanin differs from the three others through the ratio between these two peaks. At the same wavenumber positions, two negative VCD bands are present for all of the compounds. Vancomycin and oritavancin have a similar band shape (S_{fg} = 0.72; Table S13), whereas dalbavancin and teicoplanin each exhibit unique VCD intensities (S_{fg} = 0.01; Table S13). Differences between the former two compounds with respect to the two latter ones can be explained by their aromatic ring content. The distinguishment between dalbavancin and teicoplanin is not immediately explainable.

Remainder: <1570 cm^{-1}. Lastly, the remainder of the spectrum holds more complicated, often delocalized, normal modes. In general, it can be split into the amide II (1480−1570 cm^{-1}) and III regions (1230−1300 cm^{-1}), containing coupled C−N stretch and N−H bending vibrational modes, the backbone skeletal stretch region (870−1150 cm^{-1}), and the region below 800 cm^{-1} containing mostly delocalized modes, O−C−N bending modes, out-of-plane N−H bending modes, out-of-plane C═O bending modes, and C−H in-plane and out-of-plane bend modes.[36] The region below 1570 cm^{-1} will be treated entirely at once. Upon inspection of the Raman spectra in both Figures 2 and S4 (Supporting Information), unique patterns are displayed by each of the compounds. For oritavancin, again a very prominent band is present around 1291 cm^{-1}, originating from two high-intensity normal modes that involve vibrations localized on the chlorobiphenylmethyl moiety, which are absent in the case of vancomycin and dalbavancin. The ROA spectra of vancomycin and oritavancin are highly similar (S_{fg} = 0.79; Table S15). Dalbavancin displays a unique ROA pattern (S_{fg} = 0.44 with respect to vancomycin and S_{fg} = 0.34 with respect to oritavancin; Table S15). Although there are many vibrational modes overlapping in the spectral region below 1570 cm^{-1} originating from all chemical

https://doi.org/10.1021/acsomega.2c04584
ACS Omega 2022, 7, 43657−43664

entities present in the (lipo)glycopeptides, the vibrations from the aromatic rings tend to dominate the ROA spectrum.[24] Here, we see the result of how the aromatic rings, when equal in amount and conformational constellation, yield comparable ROA spectra. The conformational flexibility of the chlorobiphenylmethyl moiety renders it invisible in the ROA spectrum, along the expectations.[35]

Unique features are present in the IR spectra of each of the compounds under 1570 cm^{-1} but are much more subtle. More obvious differences can be observed in the VCD spectra. The spectra for vancomycin and oritavancin exhibit a +/0/+/− pattern between 1400 and 1500 cm^{-1}, whereas dalbavancin and teicoplanin follow a −/+/+/+ pattern. The same distinction can be made by looking at the pattern around 1200 cm^{-1}. Vancomycin and oritavancin have VCD intensity close to zero below 1200 cm^{-1}, while the other two compounds display a strong negative intensity. A common feature for all of the compounds is a positive band above 1200 cm^{-1}, albeit slightly broader for dalbavancin and teicoplanin. For vancomycin and oritavancin, in particular, this positive band is followed by a relatively strong negative VCD intensity. Based hereon, a classification can be made like before: vancomycin and oritavancin (S_{fg} = 0.87; Table S17) versus dalbavancin and teicoplanin (S_{fg} = 0.84; Table S17).

DISCUSSION

On the ground of all of the abovementioned spectral observations, we see that the two chiroptical techniques, ROA and VCD, are capable of classifying vancomycin and oritavancin in one group, and dalbavancin and teicoplanin in another. Quantitatively, this is confirmed by overlap integrals between compounds of the same spectral group to be around 0.80, as opposed to overlap integrals of around 0.40 for compounds of a different spectral group (Tables S3 and S5). The spectral intensities are governed by the amount and precise overall conformation adopted by the shared molecular tri/tetracyclic system (see red indications in Figure 1; further referred to as the glycopeptide scaffold), of which the aromatic systems are part, as found before for vancomycin, further reinforcing conclusions drawn in previous studies.[24−26] In fact, the ROA and VCD spectra tell us that the common scaffolds of vancomycin and oritavancin are highly similar, as their experimental spectra and corresponding calculated spectra and geometries are similar (see Figure 2 and Sections S4 and S5 in the Supporting Information). Dalbavancin and teicoplanin match analogously, albeit with two additional fixed aromatic rings that are included in the molecular scaffold. The deviating chiroptical spectra of these two lipoglycopeptides are the result of the presence of additional aromatic systems, as well as the conformational changes that are induced in the molecular scaffold that all of the four compounds share between one another (see Sections S4 and S5 in the Supporting Information). The addition and/or removal of a carbohydrate entity does not play a major role in the ROA and VCD intensities, as the spectral pattern of vancomycin barely differs from that of oritavancin, and that of dalbavancin is very similar to that of teicoplanin.

The nonchiral spectroscopic techniques—Raman and IR spectroscopy—do show spectral differences between the compounds that had similar ROA and VCD spectra. Their intensities appear to respond foremost to the chemical content of each compound and respond less to the conformation adopted. This too was concluded in the past for vancomycin.[24,25] The current study hence demonstrates how they are complementary between the chiral and nonchiral spectroscopic techniques and that this is not a matter of superiority of one or the other type of spectroscopy.

Lastly, we believe that the current contribution showcases that experimental work within a certain molecular class is absolutely worthwhile. Without any calculation, one discovers valuable clues as to certain spectrum−structure/conformation relationships. Previously, the experimental spectra IR and VCD of vancomycin alone were not interpretable due to the absence of representative calculations.[25] Calculations were still not possible here, hampering the extraction of direct structure−spectrum relationships. Nevertheless, the silver lining of the presented IR and VCD spectra is that having the recordings of vancomycin and derivatives at our disposal does aid in understanding the compound(s) structurally and conformationally, irrespective of the lack of representative calculated spectra.

CONCLUSIONS

In this contribution, a VOA analysis of vancomycin and its three derivatives—oritavancin, dalbavancin, and teicoplanin—was performed. By doing so, we find closure in our journey toward uncovering the added value of VOA techniques for the conformational analysis of antibiotic glycopeptides. The principal take-home messages are: (1) glycopeptides contain certain molecular scaffolds that are highly similar, for which the conformation is determinable using ROA and VCD to a lesser extent and purely empirical, (2) the aromatic rings that are incorporated in the glycopeptide within a rigid conformation dominate the VOA intensities, and (3) the addition or removal of carbohydrates and lipid entities barely influences the VOA spectra, hampering the determination of their conformations. Thus, vancomycin and oritavancin form one VOA spectral group, and dalbavancin and teicoplanin form another one. Altogether, it has become clear in what sense VOA is applicable during the conformational analysis of the ever-growing pool of antibiotic glycopeptides. Moreover, although computations appear to provide us with all of the necessary information regarding the spectral responses toward conformations and chemical structures, we herein demonstrate that additional experimental work—here through the analysis of derivatives of a compound—is of pivotal importance for an even deeper understanding. As such, the present contribution is a proof-of-concept paper raising the interest for future VOA measurement of newly discovered or already existing (lipo)-glycopeptides, for instance eventually creating a spectral database that can be used for subcategorization. Furthermore, such a future experimental database study would greatly benefit from spectral calculations as presented in previous contributions,[24,25] allowing the determination of the conformational ensemble of each individual (lipo)glycopeptide.

ASSOCIATED CONTENT

Supporting Information

The Supporting Information is available free of charge at https://pubs.acs.org/doi/10.1021/acsomega.2c04584.

Experimental IR, VCD, Raman, and ROA spectra; experimental Raman and ROA spectra of vancomycin, oritavancin, and teicoplanin four compounds in aqueous solution and of vancomycin and oritavancin in DMSO-d_6; spectral overlap integral values; DFT-level calculated

https://doi.org/10.1021/acsomega.2c04584
ACS Omega 2022, 7, 43657−43664

geometries in DMSO and in water; and selected dihedral angle values (PDF)

AUTHOR INFORMATION

Corresponding Author

Roy Aerts − *Department of Chemistry, University of Antwerp, Antwerp 2020, Belgium;* orcid.org/0000-0002-3173-8652; Email: roy.aerts@uantwerpen.be

Authors

Jonathan Bogaerts − *Department of Chemistry, University of Antwerp, Antwerp 2020, Belgium;* orcid.org/0000-0001-8089-7759

Christian Johannessen − *Department of Chemistry, University of Antwerp, Antwerp 2020, Belgium;* orcid.org/0000-0003-2613-9476

Wouter A. Herrebout − *Department of Chemistry, University of Antwerp, Antwerp 2020, Belgium;* orcid.org/0000-0002-3167-8944

Complete contact information is available at: https://pubs.acs.org/10.1021/acsomega.2c04584

Notes

The authors declare no competing financial interest.

ACKNOWLEDGMENTS

The authors acknowledge the Flemish Supercomputing Center (VSC) for providing computing resources and support. The University of Antwerp (BOF-NOI) is acknowledged for the predoctoral scholarship of R.A.

REFERENCES

(1) McCormick, M. H.; Mcguire, J.; Pittenger, G.; et al. Vancomycin, a new antibiotic. I. Chemical and biologic properties. *Antibiot. Annu.* **1955**, *3*, 606−611.

(2) Perkins, H. R. Specificity of combination between mucopeptide precursors and vancomycin or ristocetin. *Biochem. J.* **1969**, *111*, 195−205.

(3) Nieto, M.; Perkins, H. R. Modifications of the acyl-D-alanyl-D-alanine terminus affecting complex-formation with vancomycin. *Biochem. J.* **1971**, *123*, 789−803.

(4) Williams, D. H.; Williamson, M. P.; Butcher, D. W.; Hammond, S. J. Detailed binding sites of the antibiotics vancomycin and ristocetin A: determination of intermolecular distances in antibiotic/substrate complexes by use of the time-dependent NOE. *J. Am. Chem. Soc.* **1983**, *105*, 1332−1339.

(5) Schäfer, M.; Schneider, T. R.; Sheldrick, G. M. Crystal structure of vancomycin. *Structure* **1996**, *4*, 1509−1515.

(6) Sugden, R.; Kelly, R.; Davies, S. Combatting antimicrobial resistance globally. *Nat. Microbiol.* **2016**, *1*, No. 16187.

(7) Levine, D. P. Vancomycin: a history. *Clin. Infect. Dis.* **2006**, *42*, S5−S12.

(8) Nakama, Y.; Yoshida, O.; Yoda, M.; Araki, K.; Sawada, Y.; Nakamura, J.; Xu, S.; Miura, K.; Maki, H.; Arimoto, H. Discovery of a novel series of semisynthetic vancomycin derivatives effective against vancomycin-resistant bacteria. *J. Med. Chem.* **2010**, *53*, 2528−2533.

(9) Fowler, B. S.; Laemmerhold, K. M.; Miller, S. J. Catalytic site-selective thiocarbonylations and deoxygenations of vancomycin reveal hydroxyl-dependent conformational effects. *J. Am. Chem. Soc.* **2012**, *134*, 9755−9761.

(10) Yarlagadda, V.; Konai, M. M.; Manjunath, G. B.; Ghosh, C.; Haldar, J. Tackling vancomycin-resistant bacteria with 'lipophilic−vancomycin−carbohydrate conjugates'. *J. Antibiot.* **2015**, *68*, 302−312.

(11) Gu, W.; Chen, B.; Ge, M. Design and synthesis of new vancomycin derivatives. *Bioorg. Med. Chem. Lett.* **2014**, *24*, 2305−2308.

(12) Yoganathan, S.; Miller, S. J. Structure diversification of vancomycin through peptide-catalyzed, site-selective lipidation: a catalysis-based approach to combat glycopeptide-resistant pathogens. *J. Med. Chem.* **2015**, *58*, 2367−2377.

(13) Okano, A.; Isley, N. A.; Boger, D. L. Total syntheses of vancomycin-related glycopeptide antibiotics and key analogues. *Chem. Rev.* **2017**, *117*, 11952−11993.

(14) Okano, A.; Isley, N. A.; Boger, D. L. Peripheral modifications of [Ψ [CH2NH] Tpg4] vancomycin with added synergistic mechanisms of action provide durable and potent antibiotics. *Proc. Natl. Acad. Sci. U.S.A.* **2017**, *114*, E5052−E5061.

(15) Guan, D.; Chen, F.; Faridoon; Liu, J.; Li, J.; Lan, L.; Huang, W. Design and Synthesis of Pyrophosphate-Targeting Vancomycin Derivatives for Combating Vancomycin-Resistant Enterococci. *ChemMedChem* **2018**, *13*, 1644−1657.

(16) Zhao, Z.; Yan, R.; Yi, X.; Li, J.; Rao, J.; Guo, Z.; Yang, Y.; Li, W.; Li, Y.-Q.; Chen, C. Bacteria-activated theranostic nanoprobes against methicillin-resistant Staphylococcus aureus infection. *ACS Nano* **2017**, *11*, 4428−4438.

(17) Dhanda, G.; Sarkar, P.; Samaddar, S.; Haldar, J. Battle against vancomycin-resistant bacteria: recent developments in chemical strategies. *J. Med. Chem.* **2019**, *62*, 3184−3205.

(18) Mühlberg, E.; Umstätter, F.; Kleist, C.; Domhan, C.; Mier, W.; Uhl, P. Renaissance of vancomycin: Approaches for breaking antibiotic resistance in multidrug-resistant bacteria. *Can. J. Microbiol.* **2020**, *66*, 11−16.

(19) Acharya, Y.; Dhanda, G.; Sarkar, P.; Haldar, J. Pursuit of next-generation glycopeptides: a journey with vancomycin. *Chem. Commun.* **2022**, *58*, 1881−1897.

(20) Wen, Z. Q.; Hecht, L.; Barron, L. alpha.-Helix and associated loop signatures in vibrational Raman optical activity spectra of proteins. *J. Am. Chem. Soc.* **1994**, *116*, 443−445.

(21) Wen, Z. Q.; Hecht, L.; Barron, L. *β*-Sheet and associated turn signatures in vibrational Raman optical activity spectra of proteins. *Protein Sci.* **1994**, *3*, 435−439.

(22) Zhu, F.; Tranter, G. E.; Isaacs, N. W.; Hecht, L.; Barron, L. D. Delineation of protein structure classes from multivariate analysis of protein Raman optical activity data. *J. Mol. Biol.* **2006**, *363*, 19−26.

(23) Bogaerts, J.; Aerts, R.; Vermeyen, T.; Johannessen, C.; Herrebout, W.; Batista, J. M. Tackling Stereochemistry in Drug Molecules with Vibrational Optical Activity. *Pharmaceuticals* **2021**, *14*, No. 877.

(24) Aerts, R.; Vanhove, J.; Herrebout, W.; Johannessen, C. Paving the way to conformationally unravel complex glycopeptide antibiotics by means of Raman optical activity. *Chem. Sci.* **2021**, *12*, 5952−5964.

(25) Aerts, R.; Bogaerts, J.; Herrebout, W.; Johannessen, C. Insights in the vibrational optical activity spectra of the antibiotic vancomycin in DMSO. *Phys. Chem. Chem. Phys.* **2022**, *24*, 9619−9625.

(26) Aerts, R.; Herrebout, W.; Johannessen, C. Raman optical activity of the antibiotic vancomycin bound to its biological target. *J. Raman Spectrosc.***2022** *5*31220−1226. DOI: 10.1002/jrs.6347.

(27) Van Bambeke, F. Lipoglycopeptide antibacterial agents in gram-positive infections: a comparative review. *Drugs* **2015**, *75*, 2073−2095.

(28) Butler, M. S.; Hansford, K. A.; Blaskovich, M. A.; Halai, R.; Cooper, M. A. Glycopeptide antibiotics: back to the future. *J. Antibiot.* **2014**, *67*, 631−644.

(29) Boelens, H. F.; Dijkstra, R. J.; Eilers, P. H.; Fitzpatrick, F.; Westerhuis, J. A. New background correction method for liquid chromatography with diode array detection, infrared spectroscopic detection and Raman spectroscopic detection. *J. Chromatogr. A* **2004**, *1057*, 21−30.

(30) Prowse, W. G.; Kline, A. D.; Skelton, M. A.; Loncharich, R. J. Conformation of A82846B, a glycopeptide antibiotic, complexed with its cell wall fragment: an asymmetric homodimer determined using NMR spectroscopy. *Biochemistry* **1995**, *34*, 9632−9644.

(31) Dennington, R.; Keith, T. A.; Millam, J. M. *GaussView*, version 6; Semichem Inc.: Shawnee Mission KS, 2019.
(32) Bolognino, I.; Carrieri, A.; Purgatorio, R.; Catto, M.; Caliandro, R.; Carrozzini, B.; Belviso, B. D.; Majellaro, M.; Sotelo, E.; Cellamare, S.; Altomare, C. D. Enantiomeric Separation and Molecular Modelling of Bioactive 4-Aryl-3, 4-dihydropyrimidin-2 (1 H)-one Ester Derivatives on Teicoplanin-Based Chiral Stationary Phase. *Separations* **2022**, *9*, No. 7.
(33) Frisch, M. J. et al. *Gaussiañ16*, revision A.03; Gaussian Inc.: Wallingford, CT, 2016.
(34) Mensch, C.; Barron, L. D.; Johannessen, C. Ramachandran mapping of peptide conformation using a large database of computed Raman and Raman optical activity spectra. *Phys. Chem. Chem. Phys.* **2016**, *18*, 31757−31768.
(35) Mensch, C.; Johannessen, C. The influence of the amino acid side chains on the Raman optical activity spectra of proteins. *ChemPhysChem* **2019**, *20*, 42−54.
(36) Rygula, A.; Majzner, K.; Marzec, K. M.; Kaczor, A.; Pilarczyk, M.; Baranska, M. Raman spectroscopy of proteins: a review. *J. Raman Spectrosc.* **2013**, *44*, 1061−1076.

https://doi.org/10.1021/acsomega.2c04584
ACS Omega 2022, 7, 43657−43664